The local electronic properties and formation process of titanium silicide nanostructures on Si(001)-(2 × 1)

2008 J. Phys.: Condens. Matter 20 485006

(http://iopscience.iop.org/0953-8984/20/48/485006)

J. Phys.: Condens. Matter **20** (2008) 485006 (7pp) doi:10.1088/0953-8984/20/48/485006

The local electronic properties and formation process of titanium silicide nanostructures on Si(001)-(2 × 1)

M Toramaru[1], T Iida[1], K Sato[1], S Ohno[1], K Shudo[1], Y Morikawa[2] and M Tanaka[1]

[1] Faculty of Engineering, Yokohama National University, Tokiwadai 79-5, Hodogaya-ku, Yokohama 240-8501, Japan
[2] The Institute of Scientific and Industrial Research, Osaka University, Mihogaoka 8-1, Ibaraki-shi, Osaka 567-0047, Japan

Received 1 May 2008, in final form 28 August 2008
Published 22 October 2008
Online at stacks.iop.org/JPhysCM/20/485006

Abstract
Titanium silicide island formation on an Si(001)-(2 × 1) surface was studied by means of scanning tunneling microscopy (STM) *in situ* at high temperature. Just after the start of annealing at 873 K, homogeneous nucleation occurs on the terrace, while preferential growth at the step edges was observed upon prolonged annealing. As the titanium silicide islands grow, multiple steps are formed nearby. The island size distribution was analyzed at several temperatures. Two types of $TiSi_2$ structures, namely C49 and C54, were identified from the scanning tunneling spectroscopy (STS) spectra, in accordance with first-principles calculations. There was a critical island size for the transformation of C49–C54.

1. Introduction

Investigations of metal/silicon reactivity are important for understanding silicide formation in thin film systems. Titanium disilicide ($TiSi_2$) is a material commonly used for interconnects in ultra-large-scale integrated (ULSI) circuits due to its low resistivity, thermal stability and good electrical contact properties with silicon [1, 2]. As well as wiring in conventional CMOS semiconductor devices, titanium is now considered to make good contact with the carbon nanotube family because of the relatively low work function [3, 4]. On the other hand, titanium disilicide is known to be effective for vertical alignment of nanowires grown on a silicon substrate at high temperature [5] and it can be used as a buffer layer with fast electron transfer because it is resistant to electrochemical processes and is stable against chemical vapor deposition [6, 7]. However, precise contact and alignment require high crystallinity of the silicide [8]. As the silicide segregates into islands or wires on silicon surfaces when the Ti coverage is very small [9, 10], differences in the electrical properties of silicide domains will affect the properties of nanometer-scale devices, such as tunneling junctions [11] or nanotube junctions. Thus, the growth morphology and electrical properties of each form of $TiSi_2$ at the atomic scale are very important in the fabrication of semiconductor devices.

Studies of thin films of $TiSi_2$ have shown that two structural phases can be obtained at thicknesses below 10 nm on an Si substrate, namely C54 and C49 [12]. The former is a face-centered orthorhombic form with a resistivity of 16–60 $\mu\Omega$ cm, and its thermal stability makes it suitable for use in fabricating local interconnects for gate metallization and for forming Schottky barriers [13]. The latter, metastable base-centered orthorhombic structure is often generated in growth processes at the nanometer scale, but is undesirable because of its resistivity of 60–100 $\mu\Omega$ cm [13, 14].

On a Ti-deposited surface layer, $TiSi_2$ is chiefly formed at high temperature, but it is not easy to maintain the appropriate composition and crystallinity of $TiSi_2$ [15, 16]. Silicide nanocrystals of Ti_5Si_3, Ti_5Si_4 and TiSi as well have been observed in the amorphous interlayer of Ti/Si(001) [17, 18], depending on the stoichiometry [19], and the phase transition temperature from C49 to C54 is known to be higher with decreasing thickness in the range of 5–40 nm [2, 12], as shown in figure 1. The quality of the contacts is strongly affected by the composition [20, 21] because of inhomogeneous growth [22, 23]. Therefore, it is important and challenging to avoid formation of the C49 phase and to obtain the C54 phase in nanoscale structure formation. In extremely thin films of a few nm thickness, which are required nowadays, it is not clear whether we can define the transition temperature, because

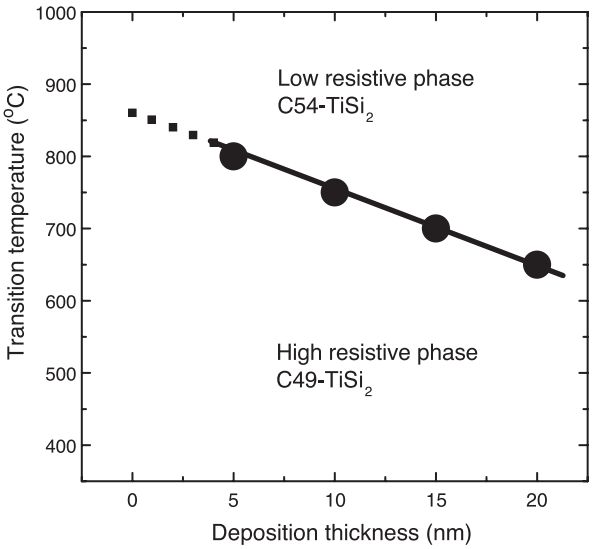

Figure 1. Phase diagram of $TiSi_2$ film with thickness of 5–40 nm. Transition temperatures from C49 to C54 on an Si(001) surface are taken from [12]. The limiting transition temperature for an extremely thin film is not known.

nanoscale islands are formed [9]. Here we describe in detail the growth of silicides at the monolayer (ML) level, based on measurements of local electronic spectra of each island.

Recently, fabrication of titanium silicide nanostructures has been demonstrated to provide useful building blocks for nanocircuits. Interconnection of titanium silicide nanowires was investigated by means of *in situ* transmission electron microscopy (TEM) [24]. Schottky barrier formation in titanium silicide nanowires on an Si(111)-(7 × 7) surface was investigated using scanning tunneling microscopy (STM) [25]. *In situ* measurement is a powerful means to understand the dynamic processes occurring at high temperatures during the growth of these novel nanostructures, since post-process investigation can lead to complex analytical hypotheses. Local electronic states evaluated by means of scanning tunneling spectroscopy (STS) can give information about individual structures, providing clues to understand the growth processes.

At the early stage of growth, a titanium atom is adsorbed on the pedestal site between Si dimers at room temperature, though it can exchange with the Si dimer at high temperatures, as shown by STM [26]. Nevertheless, the role of such diffusion in the formation of titanium silicide islands is not well understood. In our previous report, we investigated titanium silicide island formation and nearby steps on both Si(001) and Si(111) [9]. An inclined slope was observed near the islands, especially in the case of Si(001). This may indicate that the incorporation process of Si atoms into the titanium silicide islands at high temperatures is affected by the surface orientation. Here, we report the *in situ* measurement of surface morphology changes during the growth of titanium silicide on an Si(001)-(2 × 1) surface at high temperature.

Identification of the C49 phase and the C54 phase for each titanium silicide island could be crucial in identifying appropriate conditions for device fabrication. Theoretical calculations were performed for these two bulk structures [27, 28], but the spectral shape has never been thoroughly examined. In addition, although core level shifts of Si 2p in $TiSi_2$ have been discussed based on XPS measurements [29], it is very difficult to analyze the structures using XPS data [16]. On a clean Si(001) surface, scanning tunneling spectroscopy (STS) spectra in terms of $(\mathrm{d}I/\mathrm{d}V)/(I/V)$ can provide us with a fingerprint of the Si dimer site [30]. However, the spectral features of C49 and C54 are not well established. Our present results demonstrate that it is possible to identify these structures from the tunneling spectra. The obtained spectra are interpreted with the aid of first-principles calculations.

2. Experimental details

The experiments were performed with a high-temperature STM in an ultrahigh-vacuum (UHV) chamber with a base pressure of less than 1×10^{-8} Pa. Scanning tunneling microscopy/spectroscopy was performed using a JSTM-4500XT (JEOL). Electrochemically polished W tips (⌀0.5 mm) used for the STM probe were prepared in the UHV chamber by electron bombardment heating. An Si(001) wafer cut within ±0.1° from the normal (n-type, 1.0–1.2 Ω cm) was used. It was well degassed in the UHV chamber and cleaned by means of repeated cycles of heating to 1370 K. The sample was heated by applying direct current. An optical IR pyrometer was used to monitor the temperature of sample surfaces. The pressure during heating was kept below ∼3.0×10^{-8} Pa. Ti was evaporated from an electron-bombarded Ti rod (⌀0.5 mm) at the deposition rate of 0.2 ML min^{-1}. Island structures can be seen on the surface in the STM images. The average coverage of titanium on the surface was determined from the total volume of islands using the density of $TiSi_2$. Lattice parameters of $TiSi_2$ were taken from [28]. Here, 1 ML means that there are two titanium atoms in the 2 × 1 unit cell on average; this is equivalent to 6.78×10^{14} atoms cm^{-2}. Photoemission measurements were carried out using synchrotron radiation (SR) for samples prepared under the same conditions (sample, Ti evaporation source, and deposition/annealing time and temperature). In the XPS spectra, no contamination (carbon or oxygen) was apparent and the existence of Ti on the Si surface was confirmed by the observation of clear 2p peaks for both elements.

3. Theoretical calculation

Although spectra have been calculated based on the density of states in $TiSi_2$ [27, 28, 31], the spectral shapes obtained differ from each other. To interpret the observed spectra, we performed theoretical calculations with STATE (simulation tool for atom technology), which has been successfully applied for semiconductors [32], as well as transition and noble metal surfaces [33]. With this method, the origins of states can be obtained in terms of atomic orbitals. The details of the calculation have been described in [33]. The procedure employs a generalized gradient approximation (GGA) in a density functional theory (DFT) scheme, using ultrasoft pseudopotentials with a plane wave basis set. The cutoff energy

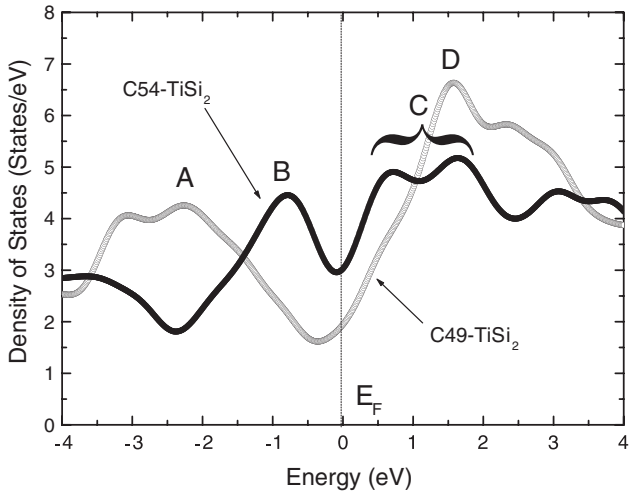

Figure 2. Theoretical calculations of density of states on C49-$TiSi_2$ and C54-$TiSi_2$ by using the program package STATE. See the text for details.

of the wavefunctions was raised to 20 Ryd, at which level the spectral shape did not change in plots. To obtain the density of states, the reciprocal space was divided into at least 15 × 15 × 15 meshes, which was more than enough to trace the spectral shape at a resolution comparable with that of STS. The lattice parameters of the bulk and the initial structures of the cells were taken from [34].

The obtained curves for C49 and C54 structures are shown in figure 2. In both structures, the density near E_F is weak. In C49, a prominent peak A at −2.1 eV consists of Si p_y and Ti d_{yz}, and that at +1.6 eV consists of Si p_x and Ti d_{z^2}. In C54, a clear peak B at −0.9 eV consists of Si p_y and Ti $d_{x^2-y^2}$, and a broad peak between +0.6 and 1.6 eV consists of Si p_z and Ti d_{yz}. These results are consistent with first-principles calculations [28], which yielded strong peaks at −2.2 and +1.6 eV for C49 (corresponding to our peaks A and D), a prominent peak at −1.0 (corresponding to our B) and a broader one between +0.9 and +1.5 eV (corresponding to our C) for C54. In their case, the broader peak of C54 is weaker than the sharper one.

4. Results and discussion

4.1. Structure observed in microscopic images

No islands of titanium silicide were formed immediately after Ti deposition at room temperature at coverages of up to one ML [9]. Figure 3 shows a series of STM images of a 0.4 ML titanium-deposited Si(001) surface after annealing at 873 K for (a) 30 s, (b) 60 s, (c) 180 s and (d) 210 s. Titanium silicide islands were formed through a thermal process. Typical islands are indicated with circles and the steps are emphasized with black curves. White dotted curves in (b) indicate where the steps were before the retreat. Rapid increase in the volumes of islands by 30–400% can be seen in (b) within

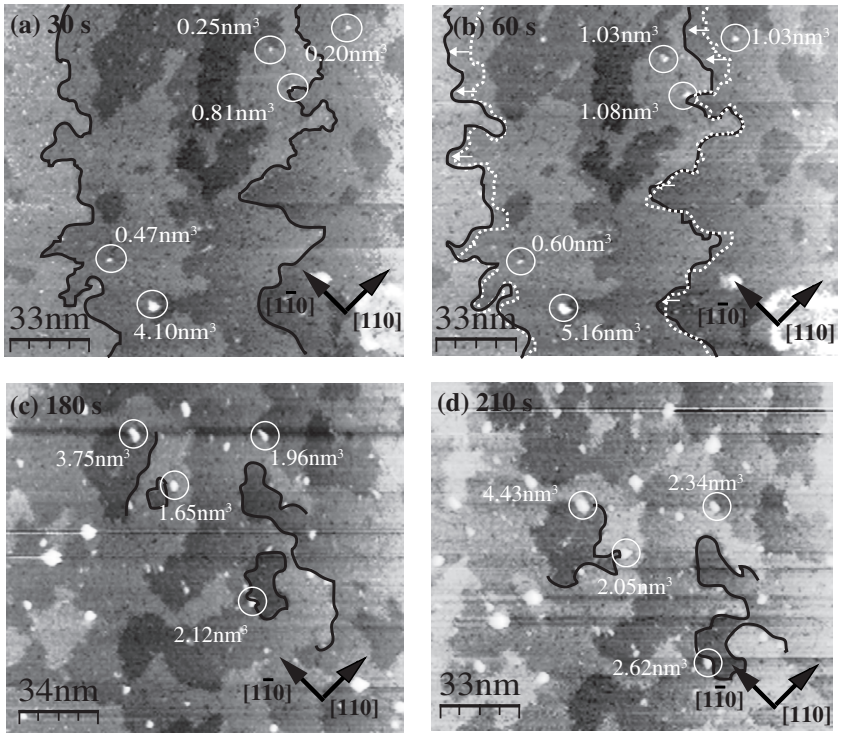

Figure 3. A series of STM images of titanium deposited on an Si(001) surface during annealing at 873 K for (a) 30 s, (b) 60 s, (c) 180 s and (d) 210 s. The solid lines in each figures show steps and the white dotted line in (b) is the same as the solid line in (a). The arrows in (b) show step retreat. The dotted line is adjusted to the most protruded position of the step line in (b) because the original position is not clear. The fusion of two holes was observed in (c) and (d). The volumes of typical islands are shown on each figure. Growth of islands is seen in (a), (b) and (c), (d). The total coverage of titanium is 0.4 ML. The size of the images is 140 × 160 nm^2 (sample bias of −2.0 V and tunneling current of 0.1 nA).

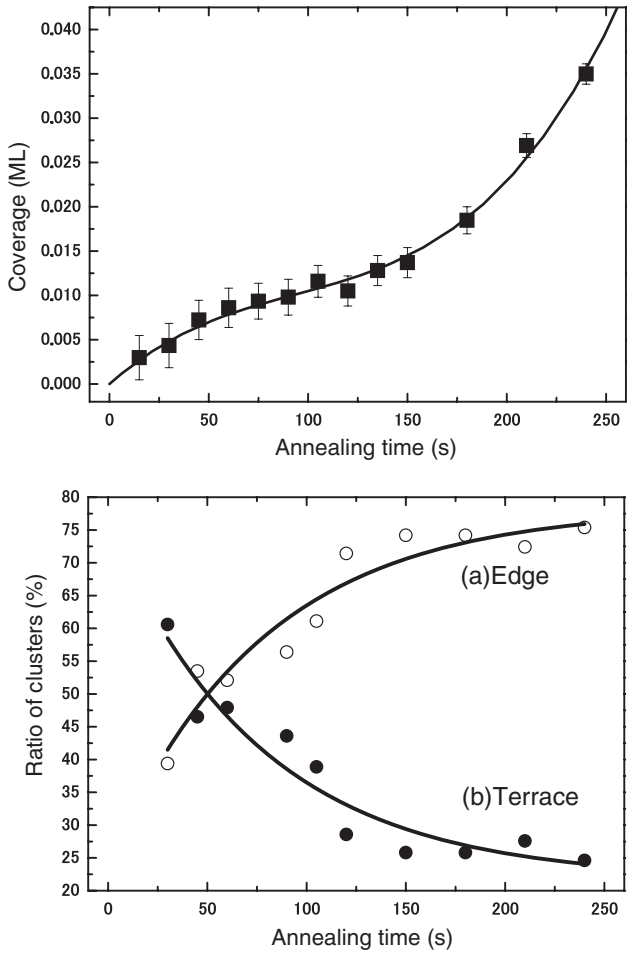

Figure 4. (a) The coverage of titanium in titanium silicide islands during annealing at 873 K when the total coverage of titanium is 0.4 ML. (b) Ratio of the islands near the step edge and at the terrace.

30 s from (a). Increase of island volumes by only ∼20–30% was observed in (c) from (d). The values of the average volume of titanium silicide islands on the Si(001) substrate are (a) 5 nm^3, (b) 7.5 nm^3, (c) 11.9 nm^3 and (d) 11.5 nm^3. In figure 3(a), titanium atoms might be distributed randomly on the terrace, although individual atoms are not well resolved. During the thermal annealing process, the number density of titanium silicide islands increased. During the growth process, the morphology of the step edges near the island becomes more ragged and the density of defects at the terrace increased. These results indicate that the Si atoms at the step edges and on the terrace are consumed to form titanium silicide islands. Most of the titanium silicide islands were formed preferentially at the step edges in figures 3(c) and (d). This means that the step is pinned at the titanium silicide islands.

We examined the ratio of titanium silicide islands at the terrace and step edges during annealing in order to clarify the dynamics of titanium silicide formation. Figure 4(a) depicts the coverage of titanium silicide during annealing at 873 K, including the experimental data in figure 3. The graph shows that there are two stages in the initial growth process. The coverage increases slowly up to 0.012 ML in 150 s, while it increases rapidly thereafter. The ratios of titanium silicide islands near the step edges and on the terrace are shown in figure 4(b). In the first stage ($t < 150$ s), the ratio of titanium silicide islands at the step edges increases rapidly to 75%. This change is predominantly the result of step retreat processes. The ratio remains almost constant in the second stage ($t > 150$ s), while the coverage of titanium silicide islands continued to increase rapidly up to 0.036 ML at 250 s. The results suggest that the island growth rate at the step edge is faster than that at the terrace. It is possible that the incorporation rate of Si is enhanced when the island is at the step edges. Island growth should occur through incorporation of both titanium and silicon atoms. Although the diffusion of individual titanium atoms would not have been resolved at high temperature, an exchange process of a titanium atom with the Si dimer [26] must also be involved.

The titanium silicide islands grew further after sufficient annealing of the sample at 873 K for 10 min as shown in figure 5(a). On the terrace, 2 × 1 dimer rows were recovered, indicating that the titanium silicide islands contained almost all the deposited titanium atoms. Although there are some defects associated with Ti atoms [35], the terrace was covered with 2 × 1 dimer rows, and STS spectra measured at the dimers looked like those of the clean surface in figure 7(a). Images were taken after subsequent annealing at 973 K for 10 min and 1073 K for 10 min, and typical cross sections of the islands are also shown. These images were recorded after the sample had cooled to room temperature. In figure 5(a), the average size and height of the islands are 34.3 nm^2 and 1.6 nm, respectively. The islands have a pyramidal shape and are mostly surrounded by multiple steps. The edges of the islands and the steps are likely to be aligned in the ⟨110⟩ direction. These multiple steps appear to consist only of Si atoms, because the step height is the same as that of a clean Si surface, although it is possible that titanium atoms may be distributed near the titanium silicide islands. The double steps are preferentially formed very near the islands, and are further surrounded by single steps as depicted in the cross section in figure 5(d). Upon annealing at 973 K, the size of the islands increases and the area of the multiple steps near the islands also increases. The average size and height of the island are 153.3 nm^2 and 1.8 nm in figure 5(b). The total volume of the islands increased further with annealing. The average volume of the islands was estimated to be almost three times larger than that in figure 5(a). Annealing at 1073 K caused a remarkable decrease in the number density of the islands. Titanium atoms may be dissolved into the bulk or evaporated at this temperature. The sizes of the titanium silicide islands formed by annealing at 873 and 973 K are shown as histograms in figure 6. The size is mostly below 100 nm^2 in the former case. The number of islands with a size over 100 nm^2 was markedly increased by annealing at 973 K. This result indicates that the diameter of ∼10 nm may be a critical size for the titanium silicide islands in terms of the crystallographic structure. To clarify this point, we performed STS measurements.

4.2. Local electronic spectra

Figure 7 shows the tunneling spectra obtained for a clean Si(001) surface and a titanium-deposited Si(001) surface. For

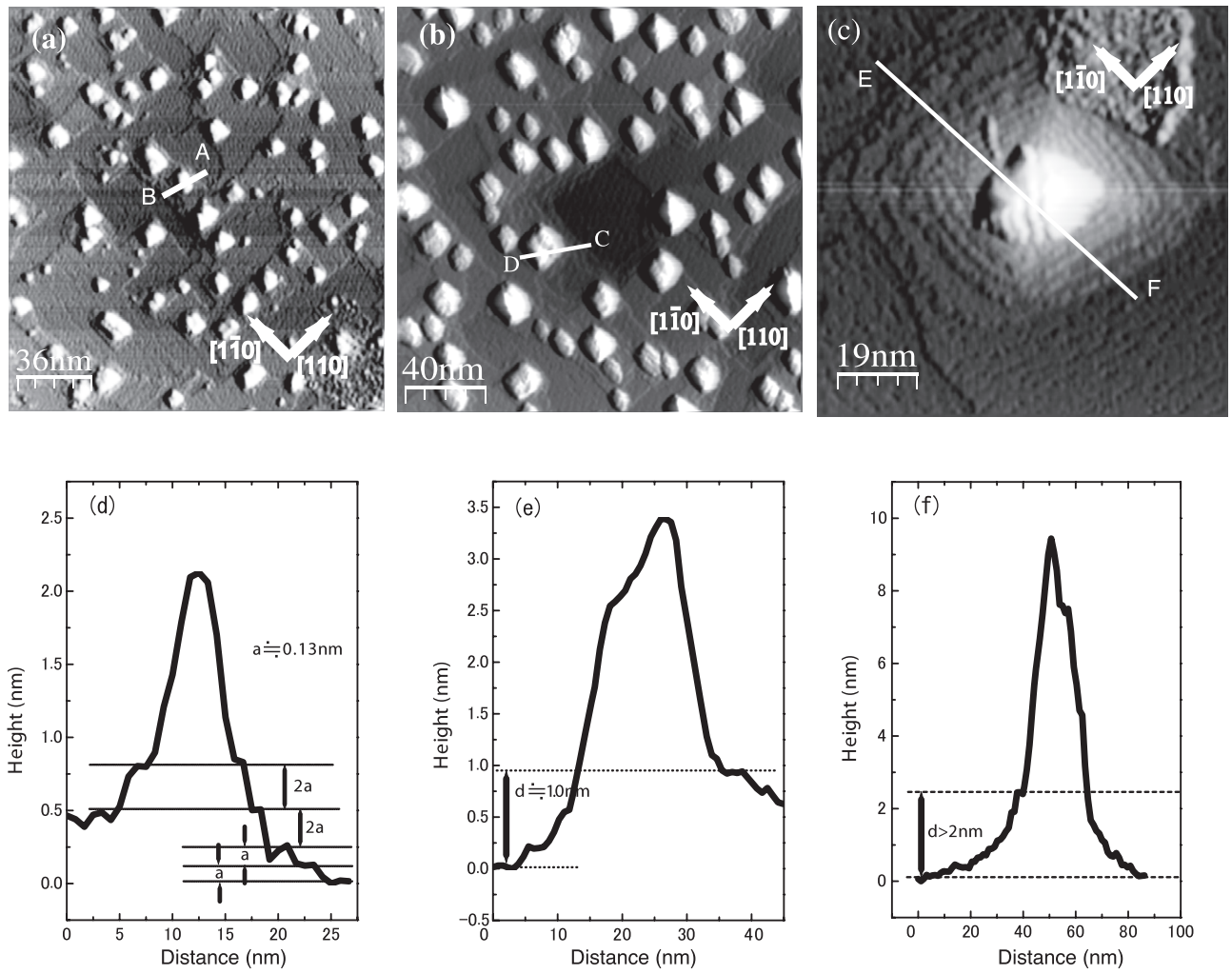

Figure 5. Filled-state STM images of titanium deposited on Si(001) recorded at room temperature after annealing at (a) 873 K for 10 min, (b) 973 K for 10 min and (c) 1073 K for 10 min. A typical cross section of a titanium silicide island is shown along the line (d) A–B in (a), (e) C–D in (b) and (f) E–F in (c).

the clean surface, three characteristic peaks were observed at −0.5 eV, +0.5 eV and +1.2 eV with respect to E_F as shown in figure 7(a). According to the literature, these are assigned to the occupied π_1 surface band, and the bottom and top of the unoccupied π_1^* surface state, respectively [30]. It should be noted that the +1.2 eV peak might be ascribed to the antibonding dimer bond (D_i^*) [36].

After titanium deposition, these peaks disappear and a peak structure is observed at −0.8 eV. This peak corresponds to the peak structure at −0.9 eV observed in an ultraviolet photoelectron spectroscopy (UPS) study of titanium deposition on sputter-cleaned Si(001) at room temperature [37]. This state appears only at low coverage and is ascribed to the hybridization of Ti 3d and Si 3p states due to weak bonding between Ti and Si dangling bonds formed at the interface [37]. It is reasonable that the state in the UPS study corresponds to the peak structure in figure 7(b) obtained just after the deposition of titanium at room temperature, because no well-crystallized silicide island was observed until after the annealing procedure. After annealing at 873 K for 10 min, figure 7(c) shows an averaged STS over the small islands. The peak at −0.8 eV in (b) disappeared and peak structures appeared at −0.4 and −2.0 eV. Unoccupied states (above E_F + 0.4 eV) had relatively higher intensity. A narrow gap indicates that the islands retain metallic character and the intensity increase at −0.4 eV suggests clustering of metallic Ti [37]. However, the enhanced peak at −2.0 eV of small islands may also represent the formation of $TiSi_2$ with a diameter of 5 nm, as is seen in the plot of density of states for C49 in figure 2 and STS in figure 7(d).

After annealing at 973 K for 10 min, typically two types of spectra were obtained, as shown by curves (d) and (e) in figure 7. Small islands with a diameter of 10 nm show a peak at −1.8 eV (d). The peak position at −1.8 eV is consistent with peak A of the calculated density of states (DOS) for C49 $TiSi_2$ in figure 2. There is a peak at −0.8 eV due to large islands with a diameter of over 20 nm (e), and this is consistent with peak B of C54 $TiSi_2$ in figure 2.

After further annealing at 1023 K, we observed the spectrum as shown in figure 7(f). This is similar to curve (e). We observed only this type of spectrum, indicating complete transformation from C49 $TiSi_2$ to C54 $TiSi_2$. Since only two

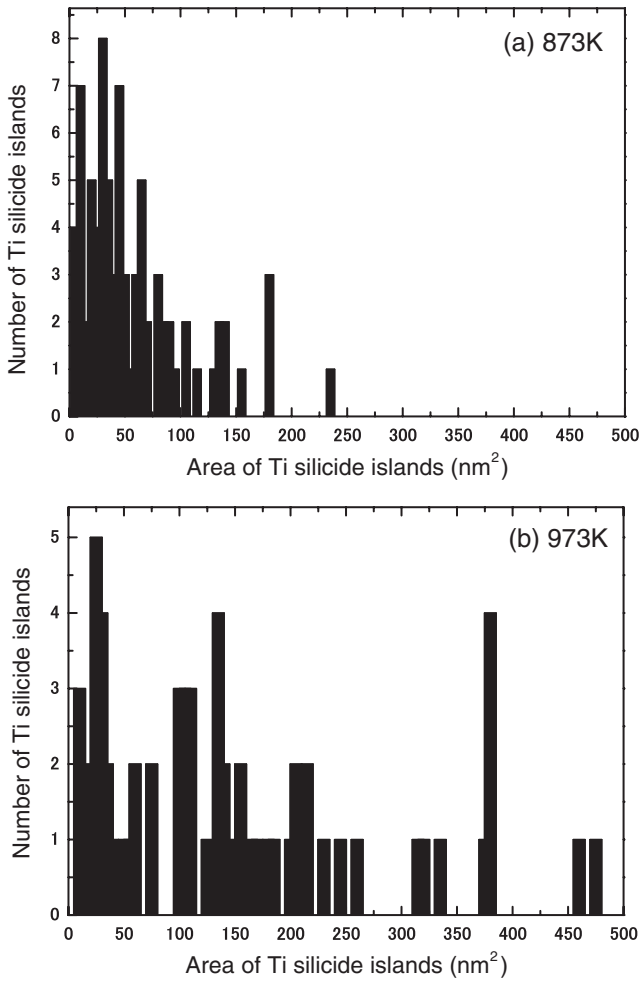

Figure 6. Histograms of the size distribution of the titanium silicide islands formed by annealing at (a) 873 K for 10 min and (b) 973 K for 10 min.

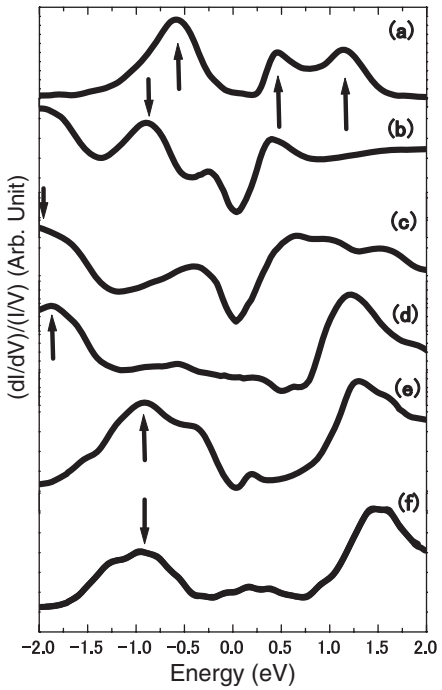

Figure 7. Typical STS spectra taken for (a) the clean surface, (b) just after titanium deposition at room temperature, (c) titanium silicide islands with a diameter of about 5 nm formed by annealing at 823 K for 10 min, (d) titanium silicide islands with a diameter of about 10 nm formed by annealing at 923 K for 10 min, (e) titanium silicide islands with a diameter of about 20 nm formed by annealing at 923 K for 10 min and (f) titanium silicide islands with a diameter of about 20 nm formed by annealing at 1023 K for 10 min.

types of spectra were observed after the annealing at 973 K, we conclude that well-crystallized $TiSi_2$ islands are formed above this temperature.

The C49 islands transform to the C54 islands by growing in volume, with a critical diameter of approximately ∼10 nm. It is possible that the same island may contain both C49 and C54 components. However, we could not find any island actually exhibiting the two types of spectra at different positions on the same island. This indicates that transformation from the C49 structure to the C54 structure occurs rapidly during the annealing process. From the viewpoint of thermodynamics, the difference in formation energy for the same amount of $TiSi_2$ in C49 and C54 structures is very small [38]. C49 is easily formed when the temperature is lower, while the islands change into C54 at very high temperature. As the surface free energies of C54 are generally larger than those of C49 [34, 39], C49 structures are preferentially formed when the islands are very small. However, when the islands grow large, they transform into C54 because the contribution of surface energy is relatively small compared to the bulk volume. The kinetics of the transformation process remains to be studied and will be further investigated by means of *in situ* measurements at high temperatures.

Finally, we should briefly mention photoemission spectroscopy. On the Ti-deposited surfaces, high intensity was seen in our UPS between −0.8 eV and E_F (results not shown here) in accordance with [37]. Heating at 873 K gave rise to a weak UPS peak between −1.9 and −2.2 eV, which is to be ascribed to the state corresponding to the STS peak in figure 7(d). After annealing at 973 K, a UPS peak at −0.7 eV appeared, but this is consistent with the dimer state of a clean Si(001) surface, because the terrace among the islands is covered with dimer rows [9]. From the XPS spectra, Si 2p components were shifted to a lower binding energy on the as-deposited surface and the surface annealed at 573 and 673 K, compared to the clean surface. This can be assigned to bond formation between Ti and Si layers [16, 37]. With increasing temperature of annealing from 873 to 1073 K, the Si $2p_{1/2}$ component shifted towards lower binding energy, indicating formation of $TiSi_2$ [29]. However, the amount of the shift is inconsistent in the literature, presumably because it might be affected by other factors, such as coverage of deposited Ti and annealing temperature. Thus, the composition of titanium silicides cannot be elucidated through the use of photoemission spectroscopy.

5. Summary

The initial growth process of titanium silicide on an Si(001)-(2 × 1) surface was observed using STM. At 873 K, small

titanium silicide islands start to grow homogeneously on the terrace. During annealing, preferential formation of titanium silicide islands occurs at the step edges, resulting in pinning of the steps. Multiple step formation was observed near titanium silicide islands after sufficient annealing. With the aid of first-principles calculations, the crystalline structures of the titanium silicide islands could be identified from STS spectra. Titanium silicide islands with a diameter below ∼10 nm corresponded to C49 $TiSi_2$, while those with a diameter over ∼10 nm corresponded to C54 $TiSi_2$. The change of island size during the annealing process was found to be a driving force for the transformation from C49 $TiSi_2$ to C54 $TiSi_2$. These findings will contribute to the improvement of fabrication processes for nanometer junctions and to the improvement of the properties of devices with silicide contacts.

Acknowledgments

We thank Dr Soh Ishii (Yokohama National University) for discussions on theoretical methods. The calculation was partly done on a workstation thanks to the courtesy of Professor Kaoru Ohno (Yokohama National University), and partly on facilities of the Supercomputer Center in joint use with the Institute for Solid State Physics, University of Tokyo. This work was supported in part by the Nippon Sheet Glass Foundation for Materials Science and Engineering.

References

[1] Bhaskaran M, Sriram S, Mitchell D R G and Holland A S 2008 *Semicond. Sci. Technol.* **23** 035021 and references therein
[2] Zhang S-L and Östling M 2003 *Crit. Rev. Solid State Mater. Sci.* **28** 1
[3] Nosho Y, Ohno Y, Kishimoto S and Mizutani T 2006 *Nanotechnology* **17** 3412–5
[4] Meng T, Wang C-Y and Wang S-Y 2007 *J. Appl. Phys.* **102** 013709
[5] Chuang C-C, Liu W-L, Chen W-J and Huang J-J 2008 *Surf. Coat. Technol.* **202** 2121
[6] Huan J H, Chen Y S, Chuang C C, Wang Y M and Kang W P 2005 *J. Vac. Sci. Technol.* B **23** 805
[7] Fang W-C, Huang J H, Sun C-L, Chen L-C, Papakoonstantinou P and Chen K-H 2006 *J. Vac. Sci. Technol.* B **24** 87
[8] Hong I-H, Chiou J W, Wang S-C, Klauser R, Pong W F, Chen L C and Chuang T J 2003 *J. Physique* IV **104** 467
[9] Iida T, Koma M, Ohwa Y, Shudo K, Ohno S and Tanaka M 2007 *Surf. Sci.* **601** 4444
[10] Ezoe K, Kuriyama H, Yamamoto T, Ohara S and Matsumoto S 1998 *Surf. Sci.* **130–132** 13–7
[11] Oh J, Meunier V, Ham H and Nemanich R J *J. Appl. Phys.* **92** 3332–7
[12] Jeon H, Yoon G and Nemanich R J 1997 *Thin Solid Films* **299** 178
[13] Ilango S, Raghavan G, Kalavathi S, Panigrahi B K and Tyagi A K 2005 *J. Appl. Phys.* **98** 073503
[14] DiGregorio J F and Wall R N 2000 *IEEE Trans. Electron Devices* **47** 313
[15] Yeh C L, Wang H J and Chen W H 2008 *J. Alloys Compounds* **450** 200
[16] del Giudice M, Joyce J J, Ruckman M W and Weaver J H 1987 *Phys. Rev.* B **35** 6213
[17] Yang T H, Chi K S and Chen L J 2005 *J. Appl. Phys.* **98** 034302
[18] Cockeram B and Wang G 1995 *Thin Solid Films* **269** 57
[19] Yeh C L, Wang H J and Chen W H 2008 *J. Alloys Compounds* **450** 200
[20] Kawade K, Suzuki A and Tanaka K 2000 *J. Phys. Soc. Japan* **69** 777
[21] Šatka A, Liday J, Srnánek R, Vincze A, Donoval D, Kováč J, Veselý M and Michalka M 2006 *Microelectron. J.* **37** 1389
[22] Via F L, Raineri V, Grimaldi M G, Miglio L, Lannuzzi M, Marabelli F, Bocelli S, Santucci S and Phani A R 2000 *J. Vac. Sci. Technol.* B **18** 721
[23] Bhaskaran M, Sriram S, Short K T, Mitchell D R G, Holland A S and Reeves G K 2007 *J. Phys. D: Appl. Phys.* **40** 5213
[24] Hsu H-C, Wu W-W, Hsu H-F and Chen L-J 2007 *Nano Lett.* **7** 885
[25] Soubiron T, Stiufiuc R, Patout L, Deresmes D, Grandidier B, Stiévenard D, Köble J and Maier M 2007 *Appl. Phys. Lett.* **90** 102112
[26] Ishiyama K and Taga Y 1995 *Phys. Rev.* B **51** 2380
[27] Wallart X, Nys J P, Zeng H S, Dalmai G, Lefebvre I and Lannoo M 1990 *Phys. Rev.* B **41** 3087
[28] Mattheiss L F and Hensel J C 1989 *Phys. Rev.* B **39** 7754
[29] Larciprete R, Danailov M, Barinov A, Gregoratti L and Kiskinova M 2001 *J. Appl. Phys.* **90** 4361
[30] Yokoyama T and Takayanagi K 2000 *Phys. Rev.* B **61** R5078
[31] Ekman M and Ozoliņš V 1998 *Phys. Rev.* B **57** 4419
[32] Morikawa Y 2001 *Phys. Rev.* B **63** 033405
[33] Hayashi T, Morikawa Y and Nozoe H 2001 *J. Chem. Phys.* **114** 7615
[34] Wang T, Oh S-Y, Lee W-J, Kim Y-J and Lee H-D 2006 *Appl. Surf. Sci.* **252** 4943
[35] Ishiyama K, Taga Y and Ichimiya A 1994 *Hyoumen-Kagaku* **16** 21
Ishiyama K, Taga Y and Ichimiya A 1996 *Surf. Sci.* **357/358** 28
[36] Hata K, Shibata Y and Shigekawa H 2001 *Phys. Rev.* B **64** 235310
[37] Arranz A and Palacio C 2005 *Surf. Sci.* **588** 92
[38] Shao G 2005 *Acta Mater.* **53** 3729
[39] Iannuzzi M and Miglio L 2001 *Surf. Sci.* **479** 201–12